*Inorg. Chem.* **2006**, *45*, 8950–8957


# Mixed-Valent Cobalt Spin Clusters: a Hexanuclear Complex and a One-Dimensional Coordination Polymer Comprised of Alternating Hepta- and Mononuclear Fragments

**Kerwyn G. Alley,[†] Roland Bircher,[‡] Oliver Waldmann,[‡] Stefan T. Ochsenbein,[‡] Hans U. Güdel,[‡] Boujemaa Moubaraki,[§] Keith S. Murray,[§] Felix Fernandez-Alonso,[||] Brendan F. Abrahams,[†] and Colette Boskovic*[,†]**

*School of Chemistry, University of Melbourne, Victoria 3010, Australia, Departement für Chemie und Biochemie, Universität Bern, Freiestrasse 3, Bern CH-3012, Switzerland, School of Chemistry, Building 23, Monash University, Clayton, Victoria 3800, Australia, and ISIS Department, Rutherford Appleton Laboratory, Chilton, Didcot OX11 0QX, U.K.*

Received May 30, 2006

Reactions between $Co(OAc)_2$ and 2-amino-2-methyl-1,3-propanediol ($ampdH_2$) afford a hexanuclear complex $[Co_6(H_2O)(MeOH)(OAc)_6(ampd)_4]$ (**1**) and a one-dimensional coordination polymer comprised of discrete heptanuclear complexes covalently bound to mononuclear Co centers $[Co_8(H_2O)_2(OAc)_7(ampd)_6]_n$ (**2**). While **1** is obtained under ambient reaction conditions, the formation of **2** requires solvothermal methods. Both products have been characterized crystallographically and found to be mixed-valent, containing divalent and trivalent Co centers. Down to 30 K, the variable-temperature magnetic susceptibility data of **1** and **2** are dominated by the single-ion properties of high-spin $Co^{II}$ centers with distorted-octahedral coordination geometries. Below this temperature, the effect of intramolecular ferromagnetic exchange interactions becomes apparent. The ferromagnetic coupling in **1** has been analyzed in terms of an anisotropic exchange model, and inelastic neutron scattering data are consistent with the proposed model. Although the structure of **2** precludes a quantitative interpretation, the magnetic data suggest ferromagnetic exchange within the heptanuclear unit and negligible interactions along the chain between the hepta- and mononuclear fragments.

## Introduction

There is currently considerable interest in the synthesis of new polynuclear complexes of paramagnetic metal centers, or spin clusters, which arises in part from the potential to access new magnetic materials. A notable class of these are spin clusters that act as "single-molecule magnets" (SMMs), displaying slow magnetization relaxation at low temperature.[1] The energy barrier to magnetization reversal responsible for this slow relaxation arises from the molecular properties of a large ground-state spin and an easy-axis (Ising) type magnetic anisotropy. The incorporation of multiple paramagnetic metal centers into extended systems such as coordination polymers also has the potential to afford important new magnetic materials. Materials with structures based on Prussian Blue that display long-range magnetic ordering at room temperature are examples of these "molecule-based magnets".[2] Coordination polymers such as Prussian Blue that are based on single metal centers bridged by polydentate ligands to form extended networks are well-known.[3] However, examples that feature discrete polynuclear metal complexes as building blocks are less common.[4] Nevertheless, coordination polymers that incorporate distinct spin clusters may represent a valuable way of combining

* To whom correspondence should be addressed. E-mail: c.boskovic@unimelb.edu.au.
[†] University of Melbourne.
[‡] Universität Bern.
[§] Monash University.
[||] Rutherford Appleton Laboratory.

(1) Gatteschi, D.; Sessoli, R. *Angew. Chem., Int. Ed.* **2003**, *42*, 268 and references cited therein.
(2) (a) Holmes, S. D.; Girolami, G. S. *J. Am. Chem. Soc.* **1999**, *121*, 5593. (b) Hatlevik, Ø.; Buschmann, W. E.; Zhnag, J.; Manson, J. L.; Miller, J. S. *Adv. Mater.* **1999**, *11*, 914. (c) Verdaguer, M.; Girolami, G. S. In *Magnetism: Molecules to Materials V*; Miller, J. S., Drillon, M., Eds.; Wiley-VCH: Weinheim, Germany, 2005; p 347.
(3) (a) Robson, R. *Dalton Trans.* **2000**, 3735. (b) Janiak, C. *Dalton Trans.* **2003**, 2781. (c) James, S. L. *Chem. Soc. Rev.* **2003**, *32*, 276.
(4) Eddaoudi, M.; Moler, D. B.; Li. H.; Chen, B.; Reineke, T. M.; O'Keefe, M.; Yaghi, O. M. *Acc. Chem. Res.* **2001**, *34*, 319 and references cited therein.


10.1021/ic060938e CCC: $33.50 
Published on Web 09/30/2006

**Chart 1.** Proligand $ampdH_2$

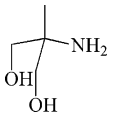


molecular-based magnetic properties (e.g., SMM behavior) with those of extended systems. Examples of this are one-dimensional coordination polymers of spin clusters that behave as "single-chain magnets" (SCMs).[5−7] SCMs are complexes with spin carriers organized into one-dimensional chains. They possess an energy barrier to magnetization reversal that results from one-dimensional Ising ferro- or ferrimagnetic behavior and gives rise to slow magnetization relaxation similar to that observed for SMMs. Although SCM behavior has not yet been reported for chain complexes of covalently bound spin clusters of nuclearity greater than three, in principle such species could act as SCMs.

We are presently investigating the coordination chemistry of the proligand 2-amino-2-methyl-1,3-propanediol ($ampdH_2$; Chart 1) and have previously reported heptanuclear Fe and tetranuclear Ni and Co spin clusters that incorporate deprotonated forms of $ampdH_2$.[8,9] A dinuclear Mo complex has also been synthesized.[10] The presence of three potential donor atoms and the multiple possible coordination modes of this ligand suggest that it is eminently suitable for the construction of new spin clusters. In addition, the tripodal conformation of the ligand appears to result in a tendency toward structures based on cuboidal units. This structural preference can enhance the likelihood of ferromagnetic exchange interactions in the resulting spin clusters, due to orthogonality of the magnetic orbitals of the paramagnetic metal centers. Such ferromagnetic interactions are desirable to achieve the high ground-state spins necessary for SMMs.

The tetranuclear Ni and Co complexes mentioned above were synthesized under ambient laboratory conditions. In the course of investigating the conditions required for the formation of these species, the hexanuclear complex reported here, $[Co_6(H_2O)(MeOH)(OAc)_6(ampd)_4]$ (**1**), was obtained. In contrast, the formation of the heptanuclear Fe complex required solvothermal conditions, and in general solvothermal methods have proved useful for synthesizing spin clusters that otherwise cannot be obtained.[11] Thus, our exploration of the chemistry of Co and $ampdH_2$ was also extended to an investigation of solvothermal syntheses, affording $[Co_8(H_2O)_2(OAc)_7(ampd)_6]_n$ (**2**), a one-dimensional coordination polymer that has a highly unusual chain structure constructed from Co-containing spin clusters alternating with mononuclear Co centers.

**Table 1.** Crystallographic Data for **1**·2.33MeOH·1.5$H_2O$ and **2**·2MeCN·2.25$H_2O$

| | **1**·2.33MeOH·1.5$H_2O$ | **2**·2MeCN·2.25$H_2O$ |
|---|---|---|
| formula | $C_{94}H_{217}Co_{18}N_{12}O_{77.5}$ | $C_{42}H_{89.5}Co_8N_8O_{30.25}$ |
| fw | 3816.54 | 1662.16 |
| space group | $P3_1$ | $C2/c$ |
| $a$, Å | 21.414(3) | 11.524(1) |
| $b$, Å | 21.414(3) | 37.727(5) |
| $c$, Å | 30.512(7) | 15.682(2) |
| α, deg | 90 | 90 |
| $\beta$, deg | 90 | 105.489(3) |
| $\gamma$, deg | 120 | 90 |
| $V$, Å$^3$ | 12117(3) | 6571(1) |
| $Z$ | 3 | 4 |
| $T$, K | 130(2) | 150(2) |
| $\rho_{calc}$, g cm$^{-3}$ | 1.569 | 1.680 |
| $\mu$, mm$^{-1}$ | 1.885 | 2.055 |
| reflns measd | 75 917 | 20 447 |
| unique reflns | 36 086 | 7456 |
| obsd data [$I > 2\sigma(I)$] | 20 951 | 5434 |
| R1[a] | 0.0846 | 0.0552 |
| wR2[b] | 0.2337 | 0.1490 |

[a] $I > 2\sigma(I)$. [b] $F^2$, all data.

## Experimental Section

**Syntheses.** All manipulations were performed under aerobic conditions, using materials as received.

**$[Co_6(H_2O)(MeOH)(OAc)_6(ampd)_4]$ (1).** Solid $Co(OAc)_2$·4$H_2O$ (3.0 g, 12 mmol) was added to a solution of $ampdH_2$ (0.84 g, 8.0 mol) in MeOH (50 cm$^3$), and the resulting mixture was stirred overnight. The filtrate was evaporated to dryness and recrystallized by layering a concentrated MeOH solution with $Et_2O$. Dark-purple hexagonal-shaped crystals formed after 3 weeks. The crystals were isolated and washed with MeOH and $Et_2O$ (60% yield). A sample for crystallography was maintained in contact with the mother liquor to prevent the loss of interstitial solvent. Drying under vacuum at room temperature afforded a fully desolvated sample. Anal. Calcd for **1**, $C_{29}H_{60}N_4Co_6O_{22}$: C, 29.75; H, 5.17; N, 4.79. Found: C, 29.84; H, 5.30; N, 4.64. However, the material appears to be hygroscopic upon standing. Anal. Calcd for **1**·5$H_2O$, $C_{29}H_{70}N_4Co_6O_{27}$: C, 27.63; H, 5.60; N, 4.44. Found: C, 27.47; H, 5.85; N, 4.39.

**$[Co_8(H_2O)_2(OAc)_7(ampd)_6]_n$ (2).** A mixture of $Co(OAc)_2$·4$H_2O$ (0.75 g, 3.0 mmol), $ampdH_2$ (0.24 g, 2.3 mmol), and MeCN (8 cm$^3$) was placed in a Teflon-lined reaction vessel and heated at 120 °C in a stainless steel bomb for 2 days. Subsequent slow cooling afforded dark-purple crystals. The crystals were isolated and washed with MeCN and MeOH (42% yield). A sample for crystallography was maintained in contact with the mother liquor to prevent the loss of interstitial solvent. Drying under vacuum afforded a fully desolvated sample. Anal. Calcd for $[Co_8(H_2O)_2(OAc)_7(ampd)_6]$, $C_{38}H_{79}N_6Co_8O_{28}$: C, 29.60; H, 5.20; N, 5.50. Found: C, 29.70; H, 5.22; N, 5.61.

**X-ray crystallography.** The intensity data of compounds **1**·2.33MeOH·1.5$H_2O$ and **2**·2MeCN·2.25$H_2O$ (Table 1) were collected on a Bruker CCD diffractometer using graphite-monochromated Mo Kα radiation ($\lambda = 0.710\ 73$ Å). Crystals were transferred directly from the mother liquor to a protective oil, which was used

(5) Ferbinteanu, M.; Miyasaka, H.; Wernsdorfer, W.; Nakata, K.; Sugira, K.; Yamashita, M.; Coulon, C.; Clerac, R. *J. Am. Chem. Soc.* **2005**, *127*, 3090 and references cited therein.

(6) (a) Caneschi, A.; Gatteschi, D.; Lalioti, N.; Sangregorio, C.; Sessoli, R.; Venturi, G.; Vindigni, A.; Rettori, A.; Pini, M. G.; Novak, M. A. *Angew. Chem., Int. Ed.* **2001**, *40*, 1760. (b) Lescouezec, R.; Vaissermann, J.; Ruiz-Perez, C.; Lloret, F.; Carrasco, R.; Julve, M.; Verdaguer, M.; Dromzee, Y.; Gatteschi, D.; Wernsdorfer, W. *Angew. Chem., Int. Ed.* **2003**, *42*, 1483. (c) Liu, T. F.; Fu, D.; Gao, S.; Zhang, Y. Z.; Sun, H. L.; Su, G.; Liu, Y. J. *J. Am. Chem. Soc.* **2003**, *125*, 13976. (d) Pardo, E.; Lloret, F.; Faus, J.; Julve, M.; Journaux, Y.; Delgado, F.; Ruiz-Perez, C. *Adv. Mater.* **2004**, *16*, 1597. (e) Ishii, N.; Ishida, T.; Mogami, T. *Inorg. Chem.* **2006**, *45*, 3837.

(7) Chakov, N. E.; Wernsdorfer, W.; Abboud, K. A.; Christou, G. *Inorg. Chem.* **2004**, *43*, 5919.

(8) Labat, G.; Boskovic, C.; Güdel, H. U. *Acta Crystallogr.* **2005**, *E61*, m611.

(9) Alley, K. G.; Bircher, R.; Güdel, H. U.; Moubaraki, B.; Murray, K. S.; Abrahams, B. F.; Boskovic, C. *Polyhedron* **2006**, doi:10.1016/j.poly.2006.06.028.

(10) McKee, V.; Wilkins, C. J. *J. Chem. Soc., Dalton Trans.* **1987**, 523.

(11) Laye, R. H.; McInnes, E. J. L *Eur. J. Inorg. Chem.* **2004**, *14*, 2811.

to prevent solvent loss. The structures were solved using direct methods and refined using a full-matrix least-squares procedure based on $F^2$ using all data.[12]

**Magnetic Measurements.** Variable-temperature magnetic susceptibility and magnetization measurements were performed with Quantum Design MPMS-XL or MPMS-5 susceptometers, each equipped with a 5-T magnet. Data were collected on powdered dried crystals restrained in eicosane or petroleum jelly to prevent torquing. Direct current (dc) susceptibility data were collected with a magnetic field of 0.1 T. Alternating current (ac) susceptibility data were collected at frequencies up to 1000 Hz on Quantum Design MPMS-XL or PPMS susceptometers.

**Inelastic Neutron Scattering (INS).** The measurements were performed on the inverted-geometry time-of-flight spectrometer IRIS at the pulsed neutron spallation source at the Rutherford Appleton Laboratory, Didcot, U.K., using the PG002 graphite analyzer with an analyzing energy of 14.8 $cm^{-1}$. Data were collected at 1.5 and 25 K and corrected for detector efficiency by means of a V reference. The time of flight to energy conversion and the data reduction were performed using the OpenGenie and MSLICE packages.[13] The instrumental resolution derived from a V metal reference at the elastic position was 0.15 $cm^{-1}$. On IRIS, the ZnS detector banks cover the angular range $2\theta = 20-160°$, giving access to a momentum transfer range $Q = 0.3-1.8$ $Å^{-1}$ at the elastic position. A fresh sample of 2 g of undeuterated **1**·$5H_2O$ was used. The sample was placed under He in an Al hollow cylinder can with an outer diameter of 23 mm and a sample thickness of 2 mm. The container was inserted in a standard ILL orange cryostat.

**Other Measurements.** IR spectra (KBr disk) were recorded on a BioRad 175 FTIR spectrometer. Elemental analyses were performed at Chemical and Microanalytical Services, Belmont, Australia.

## Results

**Syntheses.** The overnight treatment of a methanolic solution of $Co(OAc)_2$ with 0.5−1 equiv of $ampdH_2$ affords a dark-purple solution. Evaporation of this to dryness, redissolution of the residue in the minimum volume of MeOH, and layering of the resulting solution with $Et_2O$ yield crystals of **1** in 60% yield after 3 weeks. The crystals begin to degrade after a further 2 weeks if they are not removed from the mother liquor. The reaction may be formulated as

$$6Co(OAc)_2 + 4ampdH_2 + H_2O + MeOH \rightarrow [Co_6(H_2O)(MeOH)(OAc)_6(ampd)_4] + 6AcOH + 2H^+ + 2e^- \quad (1)$$

The solvothermal reaction of $Co(OAc)_2$ and $ampdH_2$ in a similar ratio in MeCN affords crystals of the polymeric product **2** in 42% yield after slow cooling. This reaction may be formulated as

$$8Co(OAc)_2 + 6ampdH_2 + 2H_2O \rightarrow [Co_8(H_2O)_2(OAc)_7(ampd)_6] + 9AcOH + 3H^+ + 3e^- \quad (2)$$

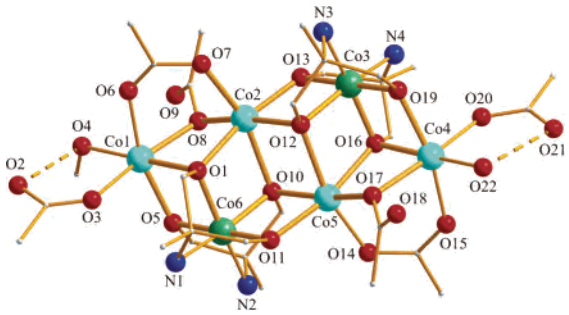


**Figure 1.** Structural representation of one of the independent molecules of complex **1** in **1**·2.33MeOH·$1.5H_2O$. Intramolecular hydrogen bonds are shown as dashed lines. Color code: $Co^{II}$, cyan; $Co^{III}$, green; O, red; N, blue; C, gray.

A similar solvothermal reaction in MeOH does not produce a crystalline product. In addition, a crystalline product cannot be isolated following workup of an analogous reaction mixture in MeCN under ambient conditions or after overnight reflux. The formation of both **1** and **2** involves partial aerial oxidation of some $Co^{II}$ centers to $Co^{III}$. As an almost immediate color change to a very dark-purple solution is observed upon mixing of the reagents, it is likely that this oxidation step occurs during the initial reaction rather than during the crystallization step. Protonation of acetate ligands and loss of acetic acid, in conjunction with double deprotonation and coordination of the $ampdH_2$ proligand, occurs during the formation of both **1** and **2**. Similar behavior is commonly observed during the synthesis of polynuclear metal complexes with mixed carboxylate and chelating alcohol/alkoxide ligands from carboxylate-containing precursors and is likely driven by the chelate effect associated with the final product.[14] It is noteworthy that the deliberate addition of base to either of the reaction mixtures prevents the isolation of crystalline products. Both **1** and **2** are major products of their respective reactions and pure, crystalline samples can be reproducibly synthesized in good yield.

**Structure Descriptions.** Compound **1**·2.33MeOH·$1.5H_2O$ crystallizes in the trigonal space group $P3_1$, with three independent hexanuclear complexes (Figure 1) per asymmetric unit, together with disordered solvent. The three complexes are not crystallographically related but are isostructural with similar metric parameters. A summary of the important interatomic distances and angles is provided in Table 2.

The $\{Co^{II}_4Co^{III}_2(\mu_2\text{-}O)_6(\mu_3\text{-}O)_4\}^{6-}$ core of **1** can be considered to be composed of four face-sharing monovacant distorted cubane units (Figure 2a), where two of the $\mu_2$-O atoms are from acetate ligands, while the remaining core O atoms are from the alkoxide arms of the four $ampd^{2-}$ ligands. The six Co atoms are essentially coplanar. Bond valence sum (BVS) calculations (Supporting Information) are consistent with four $Co^{II}$ centers (Co1, Co2, Co4, and Co5) and two $Co^{III}$ centers (Co3 and Co6).[15] The ligation is completed by the four $ampd^{2-}$ ligands, six acetate ligands, one $H_2O$ ligand,

(12) Sheldrick, G. M. *SHELX97 Programs for Crystal Structure Analysis*; Universitat Göttingen: Göttingen, Germany, 1998.
(13) Adams, M. A.; Howells, W. S.; Telling, M. T. F. *Technical Report RAL-TR-2001-002*; Rutherford Appleton Laboratory: Oxfordshire, U.K., 2001.
(14) (a) Christou, G. C. *Acc. Chem. Res.* **1989**, *22*, 328. (b) Winpenny, R. E. P. *Adv. Inorg. Chem.* **2001**, *52*, 1. (c) Brechin, E. K. *Chem. Commun.* **2005**, *41*, 5141.
(15) Brese, N. E.; O'Keefe, M. *Acta Crystallogr.* **1991**, *B47*, 192.

**Table 2.** Selected Interatomic Distances (Å) and Angles (deg) for **1**·2.33MeOH·1.5$H_2O$ and **2**·2MeCN·2.25$H_2O$

| parameter | **1**·2.33MeOH·1.5$H_2O$ | **2**·2MeCN·2.25$H_2O$ |
|---|---|---|
| $Co^{II}\cdots Co^{II}$ | 3.016(3)−3.177(3) | 3.205(1) |
| $Co^{II}\cdots Co^{III}$ | 3.002(4)−3.086(2) | 2.964(1)−3.100(1) |
| $Co^{II}-O^a$ | 1.979(9)−2.222(8) | 2.015(3)−2.260(3) |
| $Co^{III}-O^a$ | 1.854(9)−1.926(9) | 1.884(3)−1.908(3) |
| $Co^{II}-O-Co^{II}$ | 88.6(3)−94.3(3) | 94.5(1)−95.0(1) |
| $Co^{II}-O-Co^{III}$ | 94.6(4)−102.5(4) | 95.3(1)−104.9(2) |
| $O\cdots O^b$ | 2.54(1)−2.67(1) | |

[a] $\mu_3$-O and $\mu_2$-O atoms. [b] Intramolecular hydrogen bonds.

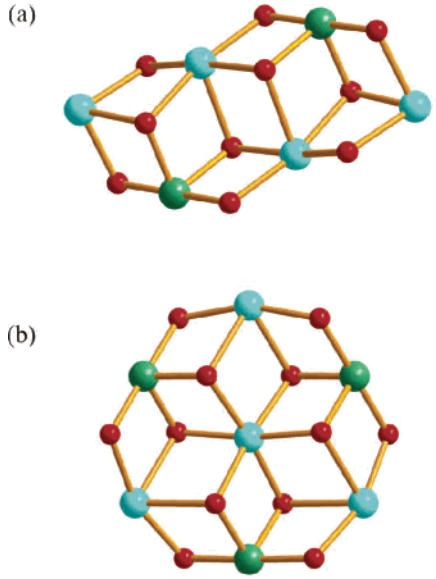


**Figure 2.** (a) $\{Co^{II}_4Co^{III}_2O_{10}\}^{6-}$ core of **1** in **1**·2.33MeOH·1.5$H_2O$. (b) $\{Co^{II}_4Co^{III}_3O_{12}\}^{7-}$ core of the heptanuclear fragment of **2** in **2**·2MeCN·2.25$H_2O$. Color code: $Co^{II}$, cyan; $Co^{III}$, green; O, red.

and a MeOH ligand. The four N atoms of the ampd$^{2-}$ ligands are all coordinated to the two $Co^{III}$ centers, and the ampd$^{2-}$ ligands bind in a $\eta^1$:$\eta^2$:$\eta^3$:$\mu_4$ fashion (Chart 2), with two above and two below the mean $Co_6$ plane. Two of the acetate ligands bridge $Co^{II}$ centers in a *syn-syn* $\eta^1$:$\eta^1$:$\mu_2$ mode, two bind in a $\eta^2$:$\mu_2$ fashion, and two bind as syn $\eta^1$ terminal ligands (Chart 2). Although the molecule formally has $C_1$ point symmetry, approximate $C_i$ symmetry exists if the mondentate $H_2O$ and MeOH ligands are ignored. Two intramolecular O−H···O hydrogen bonds are evident in the structure of **1** between the noncoordinated O atoms of the terminal acetate ligands and the MeOH and $H_2O$ ligands (Table 2). Although a number of hexanuclear Co complexes have been reported, **1** is the first Co complex to exhibit this core. However, this core unit has been observed previously in $Mn^{II}_4Mn^{III}_2$ and $Mn^{III}_6$ carboxylate complexes, with the former incorporating tripodal trialkoxide ligands and the latter containing Schiff base and methoxide ligands.[16]

Intermolecular (N−H···O) hydrogen bonds are also evident in the structure of **1** between the amine N atoms of the ampd$^{2-}$ ligands and O atoms on adjacent molecules that are

**Chart 2.** Binding Modes of (a) ampd$^{2-}$ and (b) Acetate Ligands in **1** and **2**

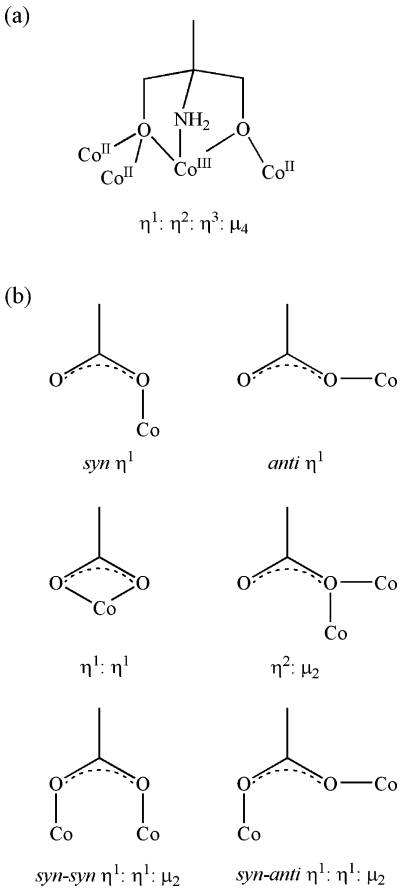


the noncoordinated O atoms from the monodentate acetate ligands or are from the $H_2O$ or MeOH ligands. This gives rise to a layered structure within the crystal, with two-dimensional sheets of H-bonded hexanuclear complexes stacked along the *c* direction.

Compound **2**·2MeCN·2.25$H_2O$ crystallizes in the monoclinic space group *C*2/*c*, with the repeat unit of the coordination polymer present in the asymmetric unit, together with disordered solvent. Complex **2** is a one-dimensional coordination polymer comprised of alternating hepta- and mononuclear moieties bridged by acetate ligands (Figure 3). A summary of the important interatomic distances and angles is provided in Table 2.

The mononuclear center Co6 is coordinated to two terminal $H_2O$ ligands, a chelating $\eta^1$:$\eta^1$ acetate ligand, and two other acetate ligands that bridge in a *syn-anti* $\eta^1$:$\eta^1$:$\mu_2$ fashion (Chart 2) to Co centers on the two adjacent heptanuclear units. The heptanuclear units contain a central Co atom and six peripheral Co atoms bridged by ampd$^{2-}$ ligands binding in the same manner that is observed in **1** (Chart 2). The $\{Co^{II}_4Co^{III}_3(\mu_2\text{-}O)_6(\mu_3\text{-}O)_6\}^{7-}$ core of this fragment (Figure 2b) can be regarded as six face-sharing monovacant distorted cubane units arranged in a cyclic fashion, with the seven Co atoms essentially coplanar. This structural motif has been observed in other heptanuclear metal complexes, where the O atoms are provided by

(16) (a) Xia, X.; Verelst, M.; Daran, J.-C.; Tuchagues, J.-P. *Chem. Commun.* **1995**, 2155. (b) Rajamaran, G.; Murugesu, M.; Sanudo, E. C.; Soler, M.; Wernsdorfer, W.; Helliwell, M.; Muryn, C.; Raftery, J.; Teat, S. J.; Christou, G. C.; Brechin, E. K. *J. Am. Chem. Soc.* **2004**, *126*, 15445.

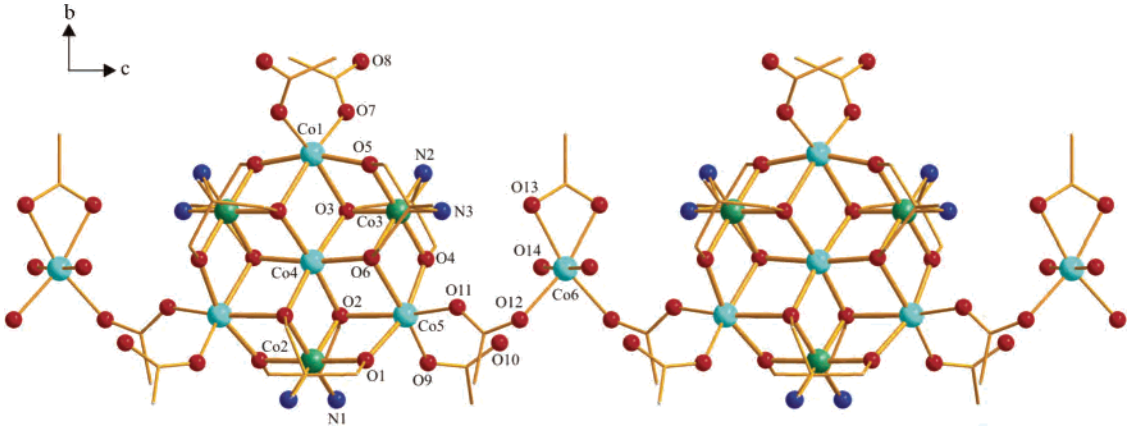


**Figure 3.** Structural representation of complex **2** in **2**·2MeCN·2.25$H_2O$. Color code: $Co^{II}$, cyan; $Co^{III}$, green; O, red; N, blue; C, gray.

hydroxo or alkoxo ligands.[17] Although this includes a heptanuclear Fe complex of $ampd^{2-}$ that we have reported previously,[8] **2** is the first Co-based example with this core unit. In **2**, as in the structurally related Fe complex, the bridging O atoms are provided by the two alkoxide arms of the $ampd^{2-}$ ligands. Three $ampd^{2-}$ ligands are located above and three below the mean $Co_7$ plane. The heptanuclear unit of **2** possesses $C_2$ point symmetry, with the $C_2$ axis passing through Co1, Co2, and Co4. BVS calculations (Supporting Information) indicate that Co1, Co4, Co5, Co5′, and Co6 are divalent while Co2, Co3, and Co3′ are trivalent. As is observed for **1**, the $Co^{III}$ atoms are coordinated to the N atoms of $ampd^{2-}$. Co1, Co5, and Co5′ are each bound to two acetate ligands. One of the acetate ligands of Co5 and Co5′ bridges to Co6, the mononuclear Co center, while the other binds in an anti $\eta^1$ terminal fashion (Chart 2). Although several coordination polymers composed of Co-containing spin clusters have been reported,[18] they do not also incorporate the mononuclear centers that make the structure of **2** so unusual.

All of the polymeric chains of **2** extend along the *c* direction within the crystal, as indicated in Figure 4. Although all chains are symmetry-related, two distinct orientations of these one-dimensional polymers are apparent (indicated in blue and red in Figure 4b). Extensive interchain hydrogen bonding results in the generation of a three-dimensional network. The two acetate ligands on Co1 hydrogen bond to the $H_2O$ ligands of Co6 (O···O distance of 2.87 Å) on an adjacent chain, linking chain A with chains C and D in Figure 4b.

It is useful to consider the structures of **1** and **2** in light of the coordination preferences of the anionic forms of the tripodal proligand $ampdH_2$. An $\eta^1{:}\eta^2{:}\eta^3{:}\mu_4$ binding mode is

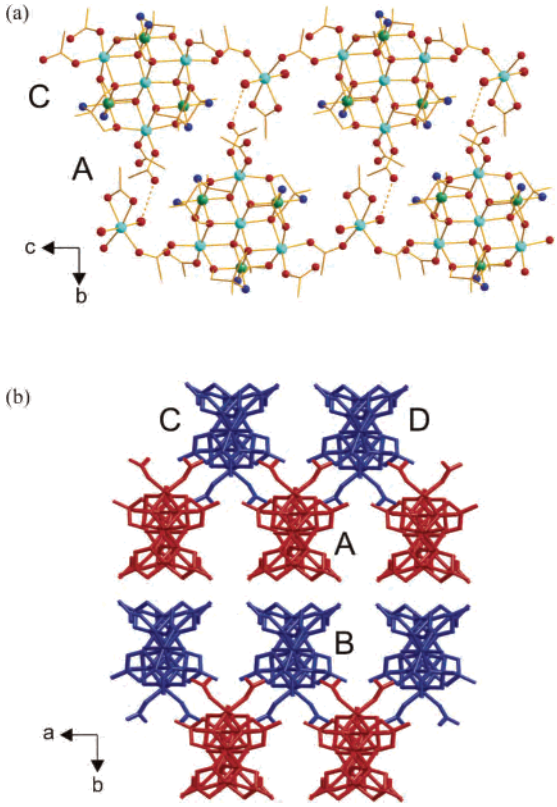


**Figure 4.** Parallel chains of **2** in **2**·2MeCN·2.25$H_2O$ extending along the *c* direction. (a) Intrachain hydrogen bonds are shown as dashed lines. (b) Red and blue chains are symmetry-related but have different orientations. Chains of the same color are related by translation.

displayed by dianionic $ampd^{2-}$ in both **1** and **2** and in the heptanuclear Fe complex that we have reported previously,[8] while a $\eta^1{:}\eta^1{:}\eta^3{:}\mu_3$ binding mode is evident for monodeprotonated $ampdH^-$ in a family of tetranuclear Ni and Co complexes.[9] All of these complexes display structures comprised of complete or monovacant distorted cubane units, and it appears that the tripodal nature of the ligand promotes these structural motifs. In addition, it is remarkable that six different binding modes are displayed by the acetate ligands in the two complexes, three of these in **1** and the other three in **2**.

**Magnetic Measurements and INS.** Variable-temperature dc magnetic susceptibility ($T = 1.8-300$ K; $H = 0.1$ T) and variable-temperature magnetization ($T = 1.8-10$ K; $H =$

(17) (a) Bolcar, M. A.; Aubin, S. M. J.; Folting, K.; Hendrickson, D. N.; Christou, G. *Chem. Commun.* **1997**, 1485. (b) Abbati, G. L.; Cornia, A.; Fabretti, A. C.; Caneschi, A.; Gatteschi, D. *Inorg. Chem.* **1998**, *37*, 3759. (c) Oshio, H.; Hoshino, N.; Ito, T.; Nakano, M.; Renz, F.; Gütlich, P. *Angew. Chem., Int. Ed.* **2003**, *42*, 223.

(18) (a) Chiang, R. K.; Huang, C. C.; Wur, C. S. *Inorg. Chem.* **2001**, *40*, 3237. (b) Li, Y. G.; Wang, E. B.; Ling, Y.; Hu, C. W.; Xu, L. *Eur. J. Inorg. Chem.* **2003**, 2567. (c) Zhou, X. G.; Han, Z. G.; Peng, J.; Chen, J. S.; Wang, E. B.; Tian, C. G.; Duan, L. Y.; Hu, N. H. *Inorg. Chem. Commun.* **2003**, *6*, 1429. (d) Yuan, D.; Xu, Y.; Hong, M.; Zhou, Y.; Li, Y. *Eur. J. Inorg. Chem.* **2005**, 1182. (e) Jones, L. F.; Jensen, P.; Moubaraki, B.; Cashion, J. D.; Berry, K. J.; Murray, K. S. *Dalton Trans.* **2005**, 3344.

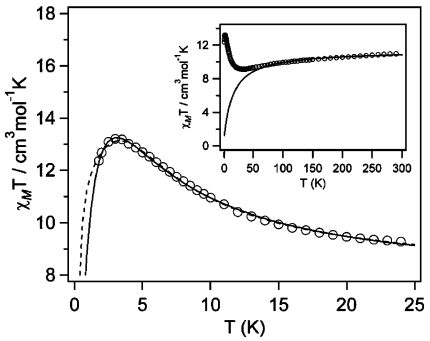


**Figure 5.** Plot of the low-temperature region of $\chi_M T$ vs $T$ ($H = 0.1$ T) for **1**·5H$_2$O. The solid and dashed lines correspond to the two best fits calculated using eq 3 and the parameter sets $J_z = 6$ K, $J_{xy} = 16$ K, $g_z = 3.9$, $g_{xy} = 4.8$ (solution 1) and $J_z = 26$ K, $J_{xy} = 2$ K, $g_z = 4.8$, $g_{xy} = 4.5$ (solution 2), respectively. The inset shows a plot of $\chi_M T$ vs $T$ for **1**·5H$_2$O over the full temperature range. The solid line corresponds to a Curie−Weiss fit with $C = 2.89$ cm$^3$ mol$^{-1}$ K per Co$^{II}$ and $\theta = -17.5$ K.

0.01−5.0 T) measurements were performed on restrained, powdered crystalline samples of compounds **1**·5H$_2$O and **2**. Both complexes are mixed-valent, and the diamagnetic low-spin Co$^{III}$ centers can be ignored in the analysis of the magnetic behavior. However, the orbital contribution to the magnetic susceptibility of octahedral Co$^{II}$ centers tends to complicate the quantitative analysis of magnetic data obtained for polynuclear Co$^{II}$ complexes.[19] The $^4T_{1g}$ ground term of high-spin distorted-octahedral Co$^{II}$ is split into six Kramers doublets by the combined effects of distortion of the octahedral crystal field and spin−orbit coupling. Fortunately, only the lowest-energy Kramers doublet is populated at low temperature ($T < 30$ K), and each Co$^{II}$ center can be treated as an effective $S_i' = {}^1/_2$ system with large anisotropy. Thus, a semiquantitative interpretation of the magnetic data may be obtained for polynuclear Co$^{II}$ species with structurally simple magnetic cores such as **1**, although this is very difficult for the structurally more complex species **2**.

The susceptibility data for **1**·5H$_2$O are plotted as $\chi_M T$ vs $T$ in the inset of Figure 5. As the temperature is decreased from 300 to 38 K, $\chi_M T$ slowly decreases from 11.0 cm$^3$ mol$^{-1}$ K to reach a shallow minimum at 9.1 cm$^3$ mol$^{-1}$ K. As the temperature is further decreased, $\chi_M T$ increases to a maximum of 13.2 cm$^3$ mol$^{-1}$ K at 3 K and then rapidly decreases at the lowest temperatures. The magnetic properties of **1** are attributed to the four octahedrally coordinated Co$^{II}$ ions, which are arranged in a chainlike fashion within the hexanuclear Co complex (Figure 2a). The room-temperature value of $\chi_M T = 11.0$ cm$^3$ mol$^{-1}$ K is considerably higher than the spin-only value of 7.5 cm$^3$ mol$^{-1}$ K calculated for four Co$^{II}$ centers ($S_i = {}^3/_2$) with $g = 2$, due to the orbital contribution. A fit of the susceptibility data to the Curie−Weiss law in the temperature range 100−300 K (solid line in the inset of Figure 5) confirms this, yielding a Curie constant $C = 2.89$ cm$^3$ mol$^{-1}$ K per Co$^{II}$ and a Curie−Weiss temperature of $\theta = -17.5$ K. Both values are typical of octahedrally coordinated Co$^{II}$ single ions.[20] The high value of $C$ (for a spin-only system with $S_i = {}^3/_2$ and $g = 2$, the calculated Curie constant is $C = 1.88$ cm$^3$ mol$^{-1}$ K) emphasizes the significant orbital contribution to the susceptibility. As the temperature is decreased, $\chi_M T$ decreases as a result of depopulation of the higher-energy Kramers doublets associated with the Co$^{II}$ single ions. Thus, in the temperature range 30−300 K, $\chi_M T$ is dominated by single-ion properties of four uncoupled Co$^{II}$ centers. However, the increase in $\chi_M T$ at temperatures below 25 K suggests intramolecular ferromagnetic exchange interactions. This is consistent with the observed Co$^{II}$−O−Co$^{II}$ bond angles of 88.6−94.3° giving rise to orthogonal magnetic orbitals.[21,22]

The exchange interactions between the four Co$^{II}$ centers in **1**·5H$_2$O can be probed in more detail by considering the low-temperature magnetic susceptibility behavior. At temperatures below 30 K, it is appropriate to describe the Co$^{II}$ centers as effective $S_i' = {}^1/_2$ spins and account for the anisotropic nature of these doublets by the introduction of anisotropic $g$ and $J$ tensors in the spin Hamiltonian. Efforts to fit the susceptibility data using isotropic $J$ values proved unsuccessful. The fully anisotropic spin Hamiltonian contains 21 parameters; however, several approximations can be made to simplify this. We have assumed the same $J$ values for the three exchange interactions (Co1···Co2, Co2···Co5, and Co4···Co5; Figure 1) and employed the same $g$ values for all four Co$^{II}$ ions. These assumptions are consistent with the minimal deviations in the structural parameters associated with the magnetic core of **1**·5H$_2$O (Table 2). Assuming axial anisotropy ($J_x = J_y = J_{xy}$; $g_x = g_y = g_{xy}$) then leads to the following effective spin Hamiltonian:[23]

$$\hat{H}'_{ex} = -\sum_{i=1}^{3}[J_{xy}(\hat{S}'_{i,x}\hat{S}'_{i+1,x} + \hat{S}'_{i,y}\hat{S}'_{i+1,y}) + J_z\hat{S}'_{i,z}\hat{S}'_{i+1,z}] + \sum_{i=1}^{4}[g_{xy}\mu_B(\hat{S}'_{i,x}H_x + \hat{S}'_{i,y}H_y) + g_z\mu_B\hat{S}'_{i,z}H_z] \quad (3)$$

The correlation of the four parameters in eq 3 with the molecular structure of **1** is not obvious. Two best-fit parameter sets were obtained from least-squares fits to the magnetic susceptibility data in the temperature range 2−25 K: $J_z = 4.5$ cm$^{-1}$, $J_{xy} = 11.4$ cm$^{-1}$, $g_z = 3.9$, $g_{xy} = 4.8$ (solution 1, solid line in Figure 5) and $J_z = 17.7$ cm$^{-1}$, $J_{xy} = 1.2$ cm$^{-1}$, $g_z = 4.8$, $g_{xy} = 4.5$ (solution 2, dashed line in Figure 5). The two fits are both of good quality, with solution 1 showing a slightly better agreement with the data in the region of the peak maximum in $\chi_M T$. To differentiate between the two solutions, isothermal magnetization data were collected at 2 K (Figure 6). The magnetization does not saturate at the high-field limit of our instrument; the experimental value at 5 T is 8.9 N$\beta$. Simulations of the

(19) (a) Kahn, O. *Molecular Magnetism*; Wiley-VCH: Weinheim, Germany, 1993; p 38. (b) Boca, R. *Struct. Bonding* **2006**, *117*, 1.
(20) Mabbs, F. E.; Machin, D. J. *Magnetism and Transition Metal Complexes*; Chapman and Hall: London, 1973; p 87.
(21) Du, M.; Guo, Y. M.; Bu, X. H.; Ribas, J. *Eur. J. Inorg. Chem.* **2004**, 3228.
(22) Berry, J. F.; Cotton, F. A.; Liu, C. Y.; Lu, T.; Murillo, C. A.; Tsukerblat, B. S.; Villagran, D. S.; Wang, X. *J. Am. Chem. Soc.* **2005**, *127*, 4895.
(23) Model fits using a spin Hamiltonian containing two different exchange interactions for the coupling between the central Co$^{II}$ ions and between central and peripheral Co$^{II}$ ions did not provide results significantly better than those obtained with eq 3.

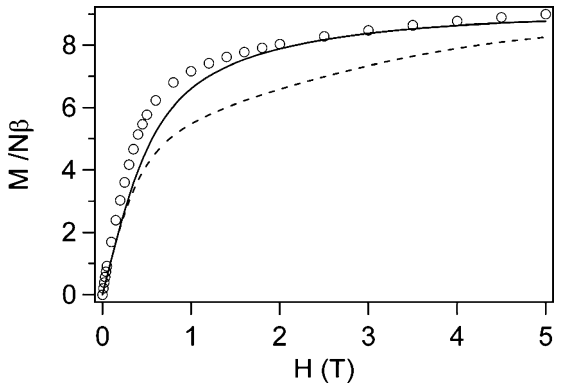


**Figure 6.** Plot of $M/N\beta$ vs $H$ at 2 K for **1**·5$H_2O$. The solid and dashed lines correspond to simulations calculated with the best-fit parameters obtained from susceptibility measurements for solutions 1 and 2, respectively (see text).

isothermal magnetization at 2 K using eq 3 are shown in Figure 6 as solid and dashed lines for the parameter sets 1 and 2, respectively. This comparison clearly favors solution 1. The agreement of the calculations with the experimental susceptibility and magnetization data is good considering the significant simplifications that were incorporated into the model. For this system, $S$ is not a good quantum number because of the large anisotropy. However, in the assumed model, $M_S$ can be used for the description of the energy levels. The solution 1 parameter set gives rise to a cluster ground state corresponding to $M_S = 0$, with an $M_S = \pm 1$ first excited state 2.0 $cm^{-1}$ above the ground state.

Further insight into the energy level scheme of **1**·5$H_2O$ can be obtained by INS.[24] INS is known to be an excellent technique for probing exchange splittings in $Co^{II}$ spin clusters, as has been shown for a series of polyoxometalate-encapsulated $Co^{II}$ compounds.[25] Figure 7 shows the INS spectra of **1**·5$H_2O$ measured at 1.5 and 25 K with an analyzing energy of 14.8 $cm^{-1}$. A comparison of the two measurements reveals inelastic intensity in the 1.5 K data in the slope to the elastic line. A background was defined on the basis of the 25 K data and subtracted from the 1.5 K data, revealing a clear peak at about 1.5 $cm^{-1}$ energy transfer (inset in Figure 7). No further magnetic transitions were detected in the measured energy-transfer window of $-1.6$ to $+10.2$ $cm^{-1}$. The program *MAGPACK*[26] was used to calculate the INS spectrum of **1**·5$H_2O$ based on the parameter set $J_{xy} = 4.5$ $cm^{-1}$ and $J_z = 11.4$ $cm^{-1}$ derived from the best fit of the susceptibility measurements (solution 1). Only one prominent transition is predicted in the energy-transfer range up to 10.2 $cm^{-1}$, corresponding to a transition from the ground state to the first excited state at 2.0 $cm^{-1}$. The agreement between calculated and measured peak positions is remarkable, providing additional credibility to the empirical Hamiltonian employed (eq 3).

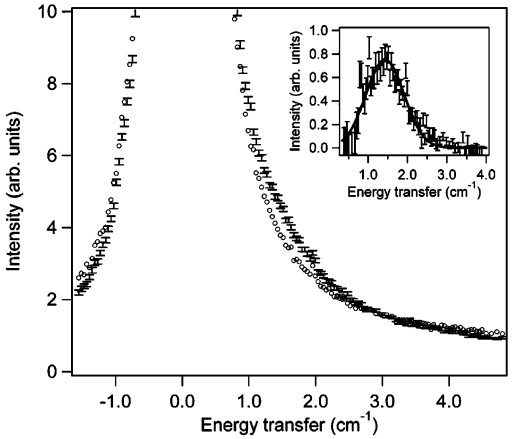


**Figure 7.** Plot of INS spectra of **1**·5$H_2O$ at 1.5 K (with error bars) and 25 K (circles). The error bars for the 25 K data are comparable to the 1.5 K data and are omitted for clarity. The inset shows the 1.5 K spectrum after correction with a background as described in the text, revealing a peak at about 1.5 $cm^{-1}$ energy transfer (fit with a Gaussian).

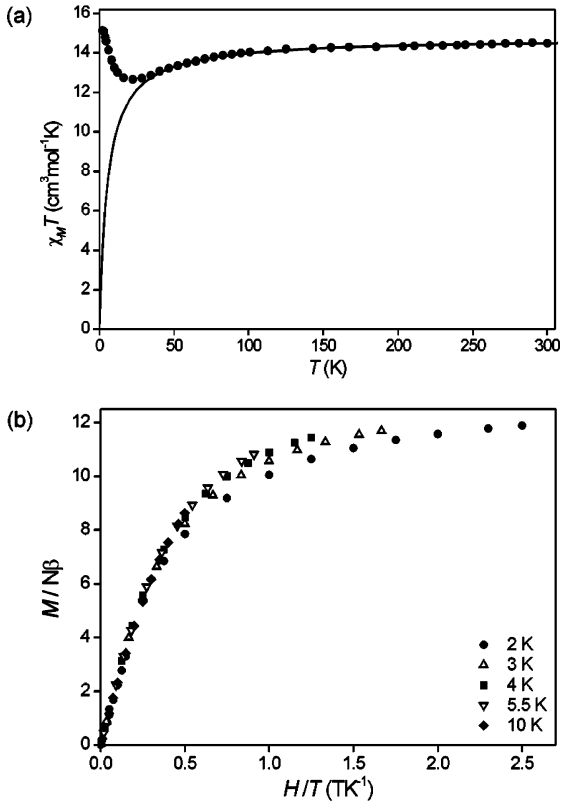


**Figure 8.** Plot of (a) $\chi_M T$ vs $T$ ($H = 0.1$ T) and (b) $M/N\beta$ vs $H/T$ for a microcrystalline sample of **2**. The solid line corresponds to a Curie−Weiss fit with $C = 2.95$ $cm^3$ $mol^{-1}$ K per $Co^{II}$ and $\theta = -5.39$ K.

The variable-temperature magnetic susceptibility and magnetization data obtained for **2** are plotted in Figure 8. At 300 K, $\chi_M T$ has a value of 14.5 $cm^3$ $mol^{-1}$ K, which remains roughly constant as the temperature is decreased to about 100 K. Below this temperature, $\chi_M T$ gradually decreases to a value of 12.7 $cm^3$ $mol^{-1}$ K at 22 K before increasing to 15.1 $cm^3$ $mol^{-1}$ K at 2 K. The overall

(24) Basler, R.; Boskovic, C.; Chaboussant, G.; Güdel, H. U.; Murrie, M.; Ochsenbein, S. T.; Sieber, A. *Chem. Phys. Chem.* **2003**, *4*, 910.
(25) (a) Clemente-Juan, J. M.; Coronado, E.; Gaita-Arino, A.; Gimenez-Saiz, C.; Güdel, H. U.; Sieber, A.; Bircher, R.; Mutka, H. *Inorg. Chem.* **2005**, *44*, 3389. (b) Andres, H.; Clemente-Juan, J. M.; Aebersold, M.; Güdel, H. U.; Coronado, E.; Buettner, H.; Kearly, G.; Melero, J.; Burriel, R. *J. Am. Chem. Soc.* **1999**, *121*, 10028. (c) Andres, H.; Clemente-Juan, J. M.; Basler, R.; Aebersold, M.; Güdel, H. U.; Borras-Almenar, J. J.; Gaita, A.; Coronado, E.; Buettner, H.; Janssen, S. *Inorg. Chem.* **2001**, *40*, 1943. (d) Clemente-Juan, J. M.; Andres, H.; Borras-Almenar, J. J.; Coronado, E.; Güdel, H. U.; Aebersold, M.; Kearly, G.; Buettner, H.; Zolliker, M. *J. Am. Chem. Soc.* **1999**, *121*, 10021.
(26) Borras-Almenar, J. J.; Clemente-Juan, J. M.; Coronado, E.; Tsukerblat, B. S. *J. Comput. Chem.* **2001**, *22*, 985.

temperature dependence of the $\chi_M T$ data for **2** is not dissimilar to that observed for **1**·5$H_2O$ and can be qualitatively interpreted in similar terms. The observed value of $\chi_M T$ at 300 K is substantially larger than the spin-only value of 9.4 $cm^3\ mol^{-1}$ K calculated for five noninteracting $Co^{II}$ ($S_i = {}^3/_2$) centers with $g = 2$, indicating a significant orbital contribution. A fit of the susceptibility data to the Curie−Weiss law in the temperature range 100−300 K (solid line in the inset of Figure 8) yields a Curie constant $C = 2.95$ $cm^3\ mol^{-1}$ K per $Co^{II}$ and a Curie−Weiss temperature of $\theta = -5.4$ K. These values are similar to the values obtained for **1**·5$H_2O$ and again emphasize the significant orbital contribution to the susceptibility. The decrease in $\chi_M T$ observed for **2** as the temperature is decreased from 100 to 22 K can also be attributed to the depopulation of higher-energy Kramers doublets of the split $^4T_{1g}$ ground state of the $Co^{II}$ single ions. The subsequent increase in $\chi_M T$ as the temperature is further decreased suggests ferromagnetic exchange interactions. In light of the structure, ferromagnetic coupling between the four $Co^{II}$ centers of the heptanuclear unit and negligible interactions between the $Co^{II}$ center of the mononuclear unit (Co5) and the other $Co^{II}$ centers seem likely. The minimum in $\chi_M T$ at 22 K is thus not due to antiferromagnetic interactions, leading to a "ferrimagnetic" arrangement of spins. In fact, the susceptibility data resemble a superposition of the behavior expected for a mononuclear $Co^{II}$ center[20] and that previously reported for a $Co^{II}_4$ complex with a very magnetic core similar to that observed in the heptanuclear unit of **2**.[21] The $Co^{II}-O-Co^{II}$ bond angles within the heptanuclear unit are 94.5−95.0°, which are similar to the bond angles associated with ferromagnetic interactions in the $Co^{II}_4$ complex, in complex **1**, and in other polynuclear complexes of $Co^{II}$.[21,22] Exchange mediated through *syn-anti* $\mu_2$ carboxylate ligands has previously been demonstrated to be weakly ferro- or antiferromagnetic,[27] and the apparently negligible interactions through this bridge in **2** are consistent with this. Although there is structural evidence for interchain hydrogen bonding, there is no indication in the magnetic data of exchange interactions through these bonds, which must be very weak and have been neglected in the above discussion.

Variable-temperature magnetization measurements were performed on **2** in the temperature range 2−10 K with fields up to 5 T (Figure 8b). The isotherms do not superimpose, and the magnetization does not saturate, with $M = 11.9\ N\beta$ at $T = 2$ K and $H = 5$ T. At these temperatures, $g' = 4.33$ for strictly octahedral $Co^{II}$ centers with $S_i' = {}^1/_2$,[19] giving a saturation value of $M = 10.9\ N\beta$ for a system with five ferromagnetically coupled or noninteracting $Co^{II}$ centers, consistent with the experimental data for **2**.

The ferromagnetic intramolecular interactions displayed by **1** and **2** imply the largest possible effective ground-state spins for hexanuclear **1** and the heptanuclear unit of **2**. Thus, ac susceptibility measurements were performed on **1**·5$H_2O$ and **2** to explore the possibility of slow magnetic relaxation due to SMM and SCM behavior, respectively. However, no peak in the out-of-phase magnetic susceptibility was observed down to 1.8 K for either compound. Several spin clusters of $Co^{II}$ have been found to act as SMMs, and SCMs with mononuclear $Co^{II}$ centers as one or both of the spin carriers have also been reported.[6,28] Nevertheless, it is quite possible that complexes **1** and **2** lack the requisite Ising-type magnetic anisotropy because the available data have not allowed the determination of this. In addition, the magnetic interaction between the poly- and mononuclear spin carriers in **2** may be too weak to give rise to SCM behavior. Co-based SMMs have previously been seen to be extremely sensitive to the effect of environmental modifications related to the loss of solvent molecules and the presence of intermolecular hydrogen bonds, which has been interpreted in terms of the effect of these features on the rate of quantum tunneling in zero field.[28] It is possible that similar phenomena could also be playing a role in the behavior observed for **1**·5$H_2O$ and **2**.

## Conclusions

The proligand ampd$H_2$ is proving to be an excellent building block for the construction of new spin clusters. A new hexanuclear Co complex and a structurally novel one-dimensional coordination polymer composed of alternating hepta- and mononuclear Co-containing fragments have been synthesized and characterized. Magnetic studies of these complexes have provided useful insights into the complex interplay between single-ion properties and exchange interactions in polynuclear $Co^{II}$ complexes. Moreover, systems that are similarly comprised of large spin clusters covalently linked into one-dimensional chains through mononuclear metal centers could represent a valuable source of new SCMs. Spin clusters that are themselves SMMs would be ideal candidates for the spin carriers in such materials, although these must be linked by ligands that can mediate exchange interactions of a reasonable magnitude.

**Acknowledgment.** Parts of this work were supported by the Australian Research Council and the Swiss National Science Foundation.

**Supporting Information Available:** Thermal ellipsoid representations of complex **1** in **1**·2.33MeOH·1.5$H_2O$ and complex **2** in **2**·2MeCN·2.25$H_2O$; selected IR data for **1** and **2**; BVS calculations for complex **1** in **1**·2.33MeOH·1.5$H_2O$ and complex **2** in **2**·2MeCN·2.25$H_2O$; X-ray crystallographic files in CIF format for **1**·2.33MeOH·1.5$H_2O$ and **2**·2MeCN·2.25$H_2O$. This material is available free of charge via the Internet at http://pubs.acs.org.

IC060938E

(27) Pei, Y.; Nakatani, K.; Kahn, O.; Sletten, J.; Renard, J. P. *Inorg. Chem.* **1989**, *28*, 3170 and references cited therein.

(28) (a) Yang, E. C.; Hendrickson, D. N.; Wernsdorfer, W.; Nakano, M.; Zakharov, L. N.; Sommer, R. D.; Rheingold, A. L.; Ledezma-Gairaud, M.; Christou, G. *J. Appl. Phys.* **2002**, *91*, 7382. (b) Murrie, M.; Teat, S. J.; Stoeckli-Evans, H.; Güdel, H. U. *Angew. Chem., Int. Ed.* **2003**, *42*, 4653. (c) Langley, S. J.; Helliwell, M.; Sessoli, R.; Rosa, P.; Wernsdorfer, W.; Winpenny, R. E. P. *Chem. Commun.* **2005**, 5029. (d) Boudalis, A. K.; Raptopolou, C. P.; Abarca, B.; Ballesteros, R.; Chadlaoui, M.; Tuchagues, J. P.; Terzis, A. *Angew. Chem, Int. Ed.* **2006**, *45*, 432.